Quantum Inf Process (2015) 14:2945–2957
DOI 10.1007/s11128-015-1019-8

Quantum limits for cascaded nondegenerate optical parametric oscillators

Wangyun Liu[1,2] · **Xiaojun Jia**[2]

Received: 29 December 2014 / Accepted: 4 May 2015 / Published online: 16 May 2015

Abstract The continuous variable multicolor entangled state of optical modes is one of the essential quantum resources for constructing quantum information networks composed of many nodes and channels. It has been well proved that the cascaded nondegenerate optical parametric oscillators (CNOPOs) are the most successful devices to produce bright entangled optical beams with different wavelengths. Here, we discuss the dependence of the possibly obtained largest-size multicolor entangled state and the entanglement degree on optical parameters of CNOPOs. Each NOPO in the cascaded system is operated above its oscillation threshold. One of two output optical beams produced by a NOPO is used for the pump light of the subsequent one, and the remained another beam serves as a submode of the multicolor entangled state. The obtainable maximal number of entangled submodes and the multicolor entanglement degree are numerically calculated under experimentally accessible conditions. The calculated results provide direct references for the design of generation systems of multicolor entangled optical beams.

Keywords Quantum entanglement · Multicolor entanglement · Cascaded nondegenerate optical parametric oscillators

✉ Xiaojun Jia
jiaxj@sxu.edu.cn

[1] School of Photoelectrical Engineering, Xi'an Technological University, Xi'an 710021, People's Republic of China

[2] State Key Laboratory of Quantum Optics and Quantum Optics Devices, Institute of Opto-Electronics, Shanxi University, Taiyuan 030006, People's Republic of China

1 Introduction

The concept of entanglement has been of great interest since the early days of quantum mechanics and has become of central importance in a variety of discussions on the fundamental aspects of quantum theory [1,2]. Nowadays, entanglement is receiving a lot of new attention in the rapidly developing quantum information science and technology [3,4]. Various continuous variable (CV) quantum information protocols, such as quantum teleportation [5], quantum key distributions [6], quantum memory of squeezed states [7,8] and quantum entanglement swapping [9], have been experimentally achieved based on utilizing optical entangled states. Different types of physical systems, for example atom ensembles [7,8], quantum dots [10] and trapped ions [11], will probably be used in nodes of a quantum network to implement information processing and storing. All these systems have own especial resonance frequencies, and thus, corresponding multicolor entangled optical beams are required to distribute entanglement and transmitting quantum information among nodes [12].

The multipartite CV entangled states with an identical frequency for all submodes have been produced by combining squeezed states of light in linear optical systems [13,14]. The multicolor entangled optical beams with several different wavelengths have been also generated by single or cascaded nondegenerate optical parametric oscillators (NOPOs) above the threshold [15–25]. In Ref. [26], the quantum limits for cascaded optical parametric amplifiers used for enhancing quantum noise reduction and efficiently producing high-quality squeezed and entangled states are theoretically analyzed. To prepare large-size multicolor entangled state with the submodes of more than three colors, we have to cascaded NOPOs more than two. In the cascaded NOPO system, one of two entangled optical beams produced by a NOPO is used for the pump light of the subsequent NOPO and quantum entanglement is transferred among all cascaded NOPOs in this way. Since the quantum fluctuation of the pump field of the subsequent NOPO depends on that of the output optical beams from the NOPO before it, the property of the multicolor entanglement generated by a cascaded system relates to the nonlinear process happened in all NOPOs. When we design the experimental system, we should comprehensively consider the operation conditions of all cascaded NOPOs and choose the cavity parameters of each NOPO to obtain the optimal multicolor entanglement.

In this paper, we theoretically analyze generation system of CV multicolor entangled state of optical modes composed by the cascaded NOPO$_k$ ($k = 1, 2, 3, \ldots, n$). Based on solving Langevin equations for the evolution of the field fluctuations inside NOPO$_k$ [24,27] and applying the sufficient condition for the quantum entanglement among amplitude and phase quadratures of optical modes proposed by van Loock and Furusawa [28], we demonstrate that the determinate CV multicolor quantum entanglement possibly exists among $n+1$ submodes produced by the n cascaded NOPOs. Since one of the output signal and idler beams from NOPO$_k$ ($k = 1, 2, 3, \ldots, n-1$), say signal, is used for the pump field of NOPO$_{k+1}$, its quantum correlation with another output beam, say idler, will directly be coupled into the signal and the idler modes of NOPO$_{k+1}$ through the intracavity nonlinear interaction. We search the limit of the number of the obtainable multicolor entangled beams under given parametric conditions of NOPO$_k$ and analyze the influences of experimental parameters on the limit with the numerical

calculation. We also discuss the dependences of the correlation variances among amplitude and phase quadratures on the pump parameters, the transmissivities of the output mirrors of NOPO$_k$ and the analysis frequency. The possible maximal cascaded number of NOPO$_k$ and the optimal cavity parameters are found. All values of the physical parameters used in the calculations are taken within the experimentally reachable regions.

The paper is organized as following. In Sect. 2, the physical system of the cascaded NOPOs is briefly described and the fundamental formulas of the field fluctuation evolution are deduced based on the Langevin equation for standard NOPOs. Then the fluctuation of the amplitude and phase quadratures of the output signal and idler fields are calculated by means of the input–output relation of NOPOs. The quantum characteristics of the multicolor entangled optical beams are numerically analyzed under given conditions in Sect. 3. In Sect. 4, the limit of the obtainable number of multicolor entangled optical beams and the dependences of the limit number on experimental parameters are analyzed through the numerical calculation. Finally, a brief summary is given in Sect. 5.

2 Description of cascaded NOPO systems

The schematic of the physical system is shown in Fig. 1. The system consists of n cascaded NOPOs. Each of NOPO$_k$ ($k = 1, 2, \ldots, n$) is composed of the input and output optical couplers, between which a type-II phase-matched $\chi^{(2)}$ nonlinear crystal is placed. The parametric interaction is enhanced by the feedback of the optical cavity, in which the three intracavity modes of signal ($\hat{a}_{1k}$), idler ($\hat{a}_{2k}$) and pump fields ($\hat{a}_{0k}$) resonate simultaneously. $\hat{a}_{0k}^{in}$ and $\hat{a}_{1k}^{in}$ ($\hat{a}_{2k}^{in}$) ($k = 1, 2, \ldots, n$) stand for the pump field amd the injected vacuum signal (idler) fields of NOPO$_k$, respectively. The output signal light $\hat{a}_{1k}^{out}$ from NOPO$_k$ ($k = 1, 2, \ldots, n-1$) is used for the pump field of the subsequent NOPO$_{k+1}$ ($\hat{a}_{1k}^{out} = a_{0,k+1}^{in}$), and the idler light $\hat{a}_{2k}^{out}$ from the NOPO$_k$ ($k = 1, 2, \ldots, n-1$) is retained as a submode of the resultant multicolor entangled states.

Using the operator linearization method, i.e., $\hat{a} = \langle\hat{a}\rangle + \delta\hat{a}$, where $\langle\hat{a}\rangle$ and $\delta\hat{a}$ are the average value and the fluctuations of the operator $\hat{a}$, respectively. The Langevin equations describing the evolution of the field fluctuations inside NOPO$_k$ ($k = 1, 2, \ldots, n$) are given by [24]

$$\begin{aligned}\tau_k \delta\dot{\hat{a}}_{0k} &= -\gamma'_{0k}\delta\hat{a}_{0k} - \sqrt{\gamma'_{0k}\gamma'_{1k}(\sigma_k - 1)}\delta\hat{a}_{1k} \\ &\quad -\sqrt{\gamma'_{0k}\gamma'_{2k}(\sigma_k - 1)}\delta\hat{a}_{2k} + \sqrt{2\gamma_{0k}}\delta\hat{a}_{0k}^{in} + \sqrt{2\mu_{0k}}\delta\hat{\beta}_{0k}^{in} \qquad (1)\\ \tau_k \delta\dot{\hat{a}}_{1k} &= \sqrt{\gamma'_{0k}\gamma'_{1k}(\sigma_k - 1)}\delta\hat{a}_{0k} - \gamma'_{1k}\delta\hat{a}_{1k} + \sqrt{\gamma'_{1k}\gamma'_{2k}}\delta\hat{a}_{2k}^{*} \\ &\quad + \sqrt{2\gamma_{1k}}\delta\hat{a}_{1k}^{in} + \sqrt{2\mu_{1k}}\delta\hat{\beta}_{1k}^{in} \qquad (2)\\ \tau_k \delta\dot{\hat{a}}_{2k} &= \sqrt{\gamma'_{0k}\gamma'_{2k}(\sigma_k - 1)}\delta\hat{a}_{0k} + \sqrt{\gamma'_{1k}\gamma'_{2k}}\delta\hat{a}_{1k}^{*} - \gamma'_{2k}\delta\hat{a}_{2k} \\ &\quad + \sqrt{2\gamma_{2k}}\delta\hat{a}_{2k}^{in} + \sqrt{2\mu_{2k}}\delta\hat{\beta}_{2k}^{in} \qquad (3)\end{aligned}$$

γ_j depends on the amplitude reflection coefficients r_j and the transmission coefficients t_j by $\gamma_j = 1 - r_j$, $\gamma_j = t_j^2/2$. μ_j relates to other intracavity loss mechanism, such as

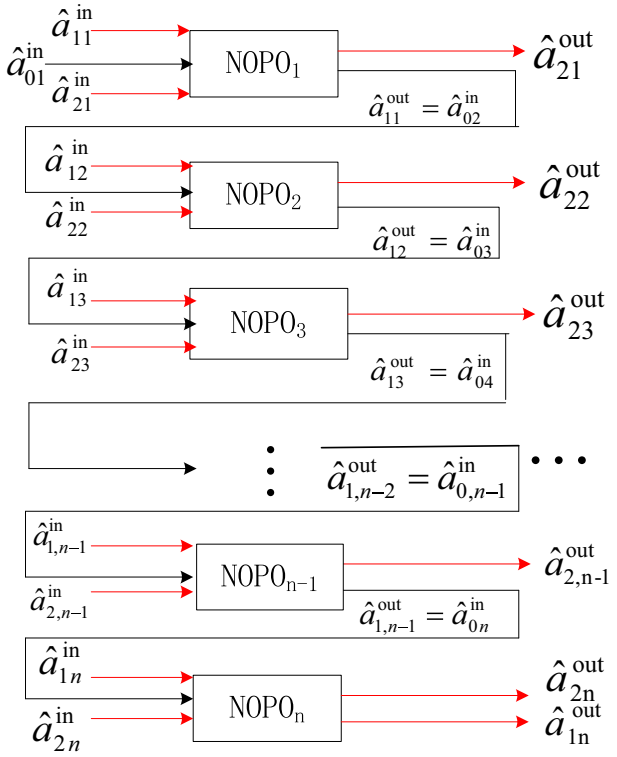

Fig. 1 The schematic of n cascaded NOPOs

the crystal absorption, surface scattering, imperfection of cavity mirrors of NOPO and so on. Combining the two loss parameters together, the total loss coefficient equals to $\gamma_j' = \gamma_j + \mu_j$. σ_k is the pump parameters of the NOPO$_k$ and $\hat{\beta}_j^{in}$ $(j = 0k, 1k, 2k)$ stands for the vacuum noises coupled to the intracavity optical modes by the internal loss mechanism inside NOPO$_k$ $(k = 1, 2, \ldots, n)$.

The amplitude $(\hat{X})$ and the phase $(\hat{Y})$ quadrature operators are defined by the field annihilation operator $\hat{a}$, i.e., $\hat{a} = e^{i\theta}(\hat{X} + i\hat{Y})$, where θ is an arbitrary phase. Generally, θ is chosen to make the average value of the imaginary of $\hat{a}$ to be zero, that is, $\langle \hat{Y} \rangle = 0$. In this case, $\hat{X}$ and $\hat{Y}$ are associated with the amplitude and the phase components of the optical field, respectively. We denote $\delta\hat{X}_j = (\delta\hat{a}_j^+ + \delta\hat{a}_j)/2$ $(j = 0k, 1k, 2k$ corresponding to the pump, signal and idler mode of NOPO$_k$, respectively) as the quadrature amplitude fluctuation of light and $\delta\hat{Y}_j = (i(\delta\hat{a}_j^+ - \delta\hat{a}_j))/2$ $(j = 0k, 1k, 2k)$ as the quadrature phase fluctuation of light. From Eqs. (1–3), we can obtain the quadrature amplitude and phase fluctuation equations of motion

$$\tau_k \frac{d\delta\hat{X}(\hat{Y})_{0k}}{dt} = -\gamma_{0k}'\delta\hat{X}(\hat{Y})_{0k} - \sqrt{\gamma_{0k}'\gamma_{1k}'(\sigma_k - 1)}\delta\hat{X}(\hat{Y})_{1k} \quad (4)$$
$$-\sqrt{\gamma_{0k}'\gamma_{2k}'(\sigma_k - 1)}\delta\hat{X}(\hat{Y})_{2k} + \sqrt{2\gamma_{0k}}\delta\hat{X}(\hat{Y})_{0k}^{in} + \sqrt{2\mu_{0k}}\delta\hat{X}(\hat{Y})_{\beta_{0k}}^{in}$$

$$\tau_k \frac{d\delta\hat{X}(\hat{Y})_{1k}}{dt} = \sqrt{\gamma'_{0k}\gamma'_{1k}(\sigma_k-1)}\delta\hat{X}(\hat{Y})_{0k} - \gamma'_{1k}\delta\hat{X}(\hat{Y})_{1k} \pm \sqrt{\gamma'_{1k}\gamma'_{2k}}\delta\hat{X}(\hat{Y})_{2k} + \sqrt{2\gamma_{1k}}\delta\hat{X}(\hat{Y})^{in}_{1k} + \sqrt{2\mu_{1k}}\delta\hat{X}(\hat{Y})^{in}_{\beta_{1k}} \quad (5)$$

$$\tau_k \frac{d\delta\hat{X}(\hat{Y})_{2k}}{dt} = \sqrt{\gamma'_{0k}\gamma'_{2k}(\sigma_k-1)}\delta\hat{X}(\hat{Y})_{0k} \pm \sqrt{\gamma'_{1k}\gamma'_{2k}}\delta\hat{X}(\hat{Y})_{1k} - \gamma'_{2k}\delta\hat{X}(\hat{Y})_{2k} + \sqrt{2\gamma_{2k}}\delta\hat{X}(\hat{Y})^{in}_{2k} + \sqrt{2\mu_{2k}}\delta\hat{X}(\hat{Y})^{in}_{\beta_{2k}} \quad (6)$$

The $\pm$ symbols in Eqs. (5) and (6) correspond to quadrature amplitude (+) and phase (−), respectively. From the Fourier transformations of Eqs. (4–6), we can get the fluctuation spectra of quadrature amplitude and phase of the intracavity modes $\hat{a}_{1k}$ and $\hat{a}_{2k}$:

$$\begin{aligned}
\delta\hat{X}_{1k}(\Omega) &= \left[\sqrt{2\gamma_{0k}}A_k^+\delta\hat{X}^{in}_{0k}(\Omega) + \sqrt{2\gamma_{1k}}K_k\delta\hat{X}^{in}_{1k}(\Omega)\right]/N_k^+ \\
&+ \left[\sqrt{2\gamma_{2k}}F_k^+\delta\hat{X}^{in}_{2k}(\Omega) + \sqrt{2\mu_{0k}}A_k^+\delta\hat{X}^{in}_{\beta_{0k}}(\Omega)\right]/N_k^+ \\
&+ \left[\sqrt{2\mu_{1k}}K_k\delta\hat{X}^{in}_{\beta_{1k}}(\Omega) + \sqrt{2\mu_{2k}}F_k^+\delta\hat{X}^{in}_{\beta_{2k}}(\Omega)\right]/N_k^+ \\
\delta\hat{X}_{2k}(\Omega) &= \left[\sqrt{2\gamma_{0k}}C_k^+\delta\hat{X}^{in}_{0k}(\Omega) + \sqrt{2\gamma_{1k}}F_k^+\delta\hat{X}^{in}_{1k}(\Omega)\right]/N_k^+ \\
&+ \left[\sqrt{2\gamma_{2k}}H_k\delta\hat{X}^{in}_{2k}(\Omega) + \sqrt{2\mu_{0k}}C_k^+\delta\hat{X}^{in}_{\beta_{0k}}(\Omega)\right]/N_k^+ \\
&+ \left[\sqrt{2\mu_{1k}}F_k^+\delta\hat{X}^{in}_{\beta_{1k}}(\Omega) + \sqrt{2\mu_{2k}}H_k\delta\hat{X}^{in}_{\beta_{2k}}(\Omega)\right]/N_k^+ \\
\delta\hat{Y}_{1k}(\Omega) &= \left[\sqrt{2\gamma_{0k}}A_k^-\delta\hat{Y}^{in}_{0k}(\Omega) + \sqrt{2\gamma_{1k}}K_k\delta\hat{Y}^{in}_{1k}(\Omega)\right]/N_k^- \\
&+ \left[\sqrt{2\gamma_{2k}}F_k^-\delta\hat{Y}^{in}_{2k}(\Omega) + \sqrt{2\mu_{0k}}A_k^-\delta\hat{Y}^{in}_{\beta_{0k}}(\Omega)\right]/N_k^- \\
&+ \left[\sqrt{2\mu_{1k}}K_k\delta\hat{Y}^{in}_{\beta_{1k}}(\Omega) + \sqrt{2\mu_{2k}}F_k^-\delta\hat{Y}^{in}_{\beta_{2k}}(\Omega)\right]/N_k^- \\
\delta\hat{Y}_{2k}(\Omega) &= \left[\sqrt{2\gamma_{0k}}C_k^-\delta\hat{Y}^{in}_{0k}(\Omega) + \sqrt{2\gamma_{1k}}F_k^-\delta\hat{Y}^{in}_{1k}(\Omega)\right]/N_k^- \\
&+ \left[\sqrt{2\gamma_{2k}}H_k\delta\hat{Y}^{in}_{2k}(\Omega) + \sqrt{2\mu_{0k}}C_k^-\delta\hat{Y}^{in}_{\beta_{0k}}(\Omega)\right]/N_k^- \\
&+ \left[\sqrt{2\mu_{1k}}F_k^-\delta\hat{Y}^{in}_{\beta_{1k}}(\Omega) + \sqrt{2\mu_{2k}}H_k\delta\hat{Y}^{in}_{\beta_{2k}}(\Omega)\right]/N_k^-
\end{aligned}$$

where

$$\begin{aligned}
A_k^\pm &= \sqrt{\gamma'_{0k}\gamma'_{1k}(\sigma_k-1)}(i\Omega+\gamma'_{2k}) \pm \sqrt{\gamma'_{0k}\gamma'_{2k}(\sigma_k-1)}\sqrt{\gamma'_{1k}\gamma'_{2k}} \\
C_k^\pm &= \sqrt{\gamma'_{0k}\gamma'_{2k}(\sigma_k-1)}(i\Omega+\gamma'_{1k}) \pm \sqrt{\gamma'_{0k}\gamma'_{1k}(\sigma_k-1)}\sqrt{\gamma'_{1k}\gamma'_{2k}} \\
F_k^\pm &= -\sqrt{\gamma'_{0k}\gamma'_{1k}(\sigma_k-1)}\sqrt{\gamma'_{0k}\gamma'_{2k}(\sigma_k-1)} \pm \sqrt{\gamma'_{1k}\gamma'_{2k}}(i\Omega+\gamma'_{0k}) \\
K_k &= (i\Omega+\gamma'_{0k})(i\Omega+\gamma'_{2k}) + \gamma'_{0k}\gamma'_{2k}(\sigma_k-1) \\
H_k &= (i\Omega+\gamma'_{0k})(i\Omega+\gamma'_{1k}) + \gamma'_{0k}\gamma'_{1k}(\sigma_k-1)
\end{aligned}$$

$$
\begin{aligned}
N_k^{\pm} = {} & (i\Omega+\gamma'_{0k})(i\Omega+\gamma'_{1k})(i\Omega+\gamma'_{2k})+(i\Omega+\gamma'_{2k})\gamma'_{0k}\gamma'_{1k}(\sigma_k-1)\\
& +(i\Omega+\gamma'_{1k})\gamma'_{0k}\gamma'_{2k}(\sigma_k-1)-(i\Omega+\gamma'_{0k})\gamma'_{1k}\gamma'_{2k}\\
& \pm 2\sqrt{\gamma'_{0k}\gamma'_{1k}(\sigma_k-1)}\sqrt{\gamma'_{0k}\gamma'_{2k}(\sigma_k-1)}\sqrt{\gamma'_{1k}\gamma'_{2k}}
\end{aligned}
$$

Using the input–output relation $\delta\hat{a}^{out}=\sqrt{2\gamma}\delta\hat{a}-\delta\hat{a}^{in}$ for an optical cavity, the fluctuations of the quadrature amplitude and phase of the output field from NOPO$_k$ are obtained in terms of their input field

$$
\begin{aligned}
\delta\hat{X}_{1k}^{out}(\Omega) = {} & \frac{2\sqrt{\gamma_{1k}\gamma_{0k}}A_k^{+}}{N_k^{+}}\delta\hat{X}_{0k}^{in}(\Omega)+\frac{2\gamma_{1k}K_k-N_k^{+}}{N_k^{+}}\delta\hat{X}_{1k}^{in}(\Omega)\\
& +\frac{\sqrt{2\gamma_{1k}}}{N_k^{+}}\Big[\sqrt{2\gamma_{2k}}F_k^{+}\delta\hat{X}_{2k}^{in}(\Omega)+\sqrt{2\mu_{0k}}A_k^{+}\delta\hat{X}_{\beta_{0k}}^{in}(\Omega)\\
& +\sqrt{2\mu_{1k}}K_k\delta\hat{X}_{\beta_{1k}}^{in}(\Omega)+\sqrt{2\mu_{2k}}F_k^{+}\delta\hat{X}_{\beta_{2k}}^{in}(\Omega)\Big] \qquad (7)\\
\delta\hat{X}_{2k}^{out}(\Omega) = {} & \frac{2\sqrt{\gamma_{2k}\gamma_{0k}}C_k^{+}}{N_k^{+}}\delta\hat{X}_{0k}^{in}(\Omega)+\frac{2\gamma_{2k}H_k-N_k^{+}}{N_k^{+}}\delta\hat{X}_{2k}^{in}(\Omega)\\
& +\frac{\sqrt{2\gamma_{2k}}}{N_k^{+}}\Big[\sqrt{2\gamma_{1k}}F_k^{+}\delta\hat{X}_{1k}^{in}(\Omega)+\sqrt{2\mu_{0k}}C_k^{+}\delta\hat{X}_{\beta_{0k}}^{in}(\Omega)\\
& +\sqrt{2\mu_{1k}}F_k^{+}\delta\hat{X}_{\beta_{1k}}^{in}(\Omega)+\sqrt{2\mu_{2k}}H_k\delta\hat{X}_{\beta_{2k}}^{in}(\Omega)\Big] \qquad (8)\\
\delta\hat{Y}_{1k}^{out}(\Omega) = {} & \frac{2\sqrt{\gamma_{1k}\gamma_{0k}}A_k^{-}}{N_k^{-}}\delta\hat{Y}_{0k}^{in}(\Omega)+\frac{2\gamma_{1k}K_k-N_k^{-}}{N_k^{-}}\delta\hat{Y}_{1k}^{in}(\Omega)\\
& +\frac{\sqrt{2\gamma_{1k}}}{N_k^{-}}\Big[\sqrt{2\gamma_{2k}}F_k^{-}\delta\hat{Y}_{2k}^{in}(\Omega)+\sqrt{2\mu_{0k}}A_k^{-}\delta\hat{Y}_{\beta_{0k}}^{in}(\Omega)\\
& +\sqrt{2\mu_{1k}}K_k\delta\hat{Y}_{\beta_{1k}}^{in}(\Omega)+\sqrt{2\mu_{2k}}F_k^{-}\delta\hat{Y}_{\beta_{2k}}^{in}(\Omega)\Big] \qquad (9)\\
\delta\hat{Y}_{2k}^{out}(\Omega) = {} & \frac{2\sqrt{\gamma_{2k}\gamma_{0k}}C_k^{-}}{N_k^{-}}\delta\hat{Y}_{0k}^{in}(\Omega)+\frac{2\gamma_{2k}H_k-N_k^{-}}{N_k^{-}}\delta\hat{Y}_{2k}^{in}(\Omega)\\
& +\frac{\sqrt{2\gamma_{2k}}}{N_k^{-}}\Big[\sqrt{2\gamma_{1k}}F_k^{-}\delta\hat{Y}_{1k}^{in}(\Omega)+\sqrt{2\mu_{0k}}C_k^{-}\delta\hat{Y}_{\beta_{0k}}^{in}(\Omega)\\
& +\sqrt{2\mu_{1k}}F_k^{-}\delta\hat{Y}_{\beta_{1k}}^{in}(\Omega)+\sqrt{2\mu_{2k}}H_k\delta\hat{Y}_{\beta_{2k}}^{in}(\Omega)\Big] \qquad (10)
\end{aligned}
$$

Since $a_{1k}^{out}=a_{0,k+1}^{in}$, $\delta\hat{X}_{0k}^{in}(\Omega)$ and $\delta\hat{Y}_{0k}^{in}(\Omega)$ in $\delta\hat{X}_{1k}^{out}(\Omega)$, $\delta\hat{X}_{2k}^{out}(\Omega)$, $\delta\hat{Y}_{1k}^{out}(\Omega)$ and $\delta\hat{Y}_{2k}^{out}(\Omega)$ can be replaced by $\delta\hat{X}_{1,k-1}^{out}(\Omega)$ and $\delta\hat{Y}_{1,k-1}^{out}(\Omega)$, all retained outputs of each NOPO$_k$, $\hat{a}_{21}^{out}(\Omega)$, $\hat{a}_{22}^{out}(\Omega)$, $\hat{a}_{23}^{out}(\Omega)$, …, $\hat{a}_{2,n-1}^{out}(\Omega)$, $\hat{a}_{2n}^{out}(\Omega)$ and $\hat{a}_{1n}^{out}(\Omega)$ can be deduced.

3 Entanglement characteristics

There are two types of the inseparability criteria for optical modes are used to verify the quantum entanglement among the obtained modes [28–30]. One criterion based on positivity under partial transposition is the sufficient and necessary condition for CV entanglement of Gaussian optical modes [29,30]. Another and more easily identified criterion is the inseparability criterion proposed by van Loock and Furusawa for optical modes in Ref. [22,28]. Here we select the second one in our theoretical analysis. When the vacuum noise of each submode is normalized to 1, it is easy to directly write the criterion inequalities of the quantum entanglement among the output submodes of the cascaded NOPO system as following:

$$\left\langle \Delta\left(\delta\hat{X}_{2k}^{out}(\Omega)-\delta\hat{X}_{2,k-1}^{out}(\Omega)\right)^2\right\rangle+\left\langle \Delta\left(\sum_{q=1}^{n}\delta\hat{Y}_{2q}^{out}(\Omega)+\delta\hat{Y}_{1n}^{out}(\Omega)\right)^2\right\rangle<4, \tag{11}$$

for $k = 2, 3, \ldots, n$, and

$$\left\langle \Delta\left(\delta\hat{X}_{1n}^{out}(\Omega)-\delta\hat{X}_{2n}^{out}(\Omega)\right)^2\right\rangle+\left\langle \Delta\left(\sum_{q=1}^{n}\delta\hat{Y}_{2q}^{out}(\Omega)+\delta\hat{Y}_{1n}^{out}(\Omega)\right)^2\right\rangle<4, \tag{12}$$

where "4" is the limit of the normalized vacuum noise. When the left side of the equations is smaller than "4," the quantum correlations exist among these quadratures. If the n inequalities in Eqs. (11) and (12) are simultaneously satisfied, the $n+1$ modes are in an inseparable entangled state [28], and thus, these inequalities give the sufficient conditions for justifying the multicolor entanglement of optical modes.

For simplicity and without losing generality, we assume that the signal and idler mode inside NOPO have the same losses and transmission factors, i.e., $\mu_{1k} = \mu_{2k} = \mu_k$, $\gamma_{1k} = \gamma_{2k} = \gamma_k$ and $\gamma'_{1k} = \gamma'_{2k} = \gamma'_k$ for each NOPO$_k$. The fluctuations of the quadrature amplitude and the quadrature phase of the output field from NOPO$_k$ in Eqs. (7–10) can be simplified as

$$\begin{aligned}\delta\hat{X}_{1k(2k)}^{out}(\Omega)&=a_k^{+}\delta\hat{X}_{0k}^{in}(\Omega)+b_k^{+}\delta\hat{X}_{1k(2k)}^{in}(\Omega)+c_k^{+}\delta\hat{X}_{2k(1k)}^{in}(\Omega)\\&\quad+d_k^{+}\delta\hat{X}_{\beta_{0k}}^{in}(\Omega)+e_k^{+}\delta\hat{X}_{\beta_{1k(2k)}}^{in}(\Omega)+f_k^{+}\delta\hat{X}_{\beta_{2k(1k)}}^{in}(\Omega)\end{aligned} \tag{13}$$

$$\begin{aligned}\delta\hat{Y}_{1k(2k)}^{out}(\Omega)&=a_k^{-}\delta\hat{Y}_{0k}^{in}(\Omega)+b_k^{-}\delta\hat{Y}_{1k(2k)}^{in}(\Omega)+c_k^{-}\delta\hat{Y}_{2k(1k)}^{in}(\Omega)\\&\quad+d_k^{-}\delta\hat{Y}_{\beta_{0k}}^{in}(\Omega)+e_k^{-}\delta\hat{Y}_{\beta_{1k(2k)}}^{in}(\Omega)+f_k^{-}\delta\hat{Y}_{\beta_{2k(1k)}}^{in}(\Omega)\end{aligned} \tag{14}$$

where, for simplicity, we denote

$$a_k^{\pm}=\frac{2\sqrt{\gamma_k\gamma_{0k}}A_k^{\pm}}{N_k^{\pm}},\ b_k^{\pm}=\frac{2\gamma_k K_k-N_k^{\pm}}{N_k^{\pm}},\ c_k^{\pm}=\frac{2\gamma_k F_k^{\pm}}{N_k^{\pm}}$$

$$d_k^{\pm} = \frac{2\sqrt{\gamma_k \mu_{0k}} A_k^{\pm}}{N_k^{\pm}}, e_k^{\pm} = \frac{2\sqrt{\gamma_k \mu_k} K_k}{N_k^{\pm}}, f_k^{\pm} = \frac{2\sqrt{\gamma_k \mu_k} F_k^{\pm}}{N_k^{\pm}}$$

Since the output signal beam from NOPO$_k$ ($k = 1, 2, \ldots, n-1$) is used for the pump field of NOPO$_{k+1}$, we can substitute $a_{1k}^{out} = a_{0,k+1}^{in}$ into equations (13–14) and get the output field expression in term of the initial input field

$$\begin{aligned}
\delta\hat{X}_{1k(2k)}^{out}(\Omega) = & \prod_{q=1}^{n} a_q^{+} \delta\hat{X}_{01}^{in}(\Omega) + \sum_{p=1}^{k-1} \prod_{q=p+1}^{k} a_q^{+} \left(b_p^{+} \delta\hat{X}_{1,p}^{in}(\Omega) + c_p^{+} \delta\hat{X}_{2,p}^{in}(\Omega) \right. \\
& \left. + d_p^{+} \delta\hat{X}_{\beta_{0,p}}^{in}(\Omega) + e_p^{+} \delta\hat{X}_{\beta_{1,p}}^{in}(\Omega) + f_p^{+} \delta\hat{X}_{\beta_{2,p}}^{in}(\Omega) \right) \\
& + b_k^{+} \delta\hat{X}_{1k(2k)}^{in}(\Omega) + c_k^{+} \delta\hat{X}_{2k(1k)}^{in}(\Omega) + d_k^{+} \delta\hat{X}_{\beta_{0k}}^{in}(\Omega) \\
& + e_k^{+} \delta\hat{X}_{\beta_{1k(2k)}}^{in}(\Omega) + f_k^{+} \delta\hat{X}_{\beta_{2k(1k)}}^{in}(\Omega) \qquad (15)
\end{aligned}$$

$$\begin{aligned}
\delta\hat{Y}_{1k(2k)}^{out}(\Omega) = & \prod_{q=1}^{n} a_q^{-} \delta\hat{Y}_{01}^{in}(\Omega) + \sum_{p=1}^{k-1} \prod_{q=p+1}^{k} a_q^{-} \left(b_p^{-} \delta\hat{Y}_{1,p}^{in}(\Omega) + c_p^{-} \delta\hat{Y}_{2,p}^{in}(\Omega) \right. \\
& \left. + d_p^{-} \delta\hat{Y}_{\beta_{0,p}}^{in}(\Omega) + e_p^{-} \delta\hat{Y}_{\beta_{1,p}}^{in}(\Omega) + f_p^{-} \delta\hat{Y}_{\beta_{2,p}}^{in}(\Omega) \right) \\
& + b_k^{-} \delta\hat{Y}_{1k(2k)}^{in}(\Omega) + c_k^{-} \delta\hat{Y}_{2k(1k)}^{in}(\Omega) + d_k^{-} \delta\hat{Y}_{\beta_{0k}}^{in}(\Omega) \\
& + e_k^{-} \delta\hat{Y}_{\beta_{1k(2k)}}^{in}(\Omega) + f_k^{-} \delta\hat{Y}_{\beta_{2k(1k)}}^{in}(\Omega) \qquad (16)
\end{aligned}$$

Generally, the initial pump light is in the coherent state, and thus, the noise variances of its quadrature amplitude and quadrature phase fluctuations should be normalized to "1," i.e., $\langle \Delta[\delta\hat{X}_{01}^{in}(\Omega)]^2 \rangle = \langle \Delta[\delta\hat{Y}_{01}^{in}(\Omega)]^2 \rangle = 1$. In each NOPO, the vacuum noise is also injected into the signal and idler mode, i.e., $\langle \Delta[\delta\hat{X}_{1k}^{in}(\Omega)]^2 \rangle = \langle \Delta[\delta\hat{X}_{2k}^{in}(\Omega)]^2 \rangle = \langle \Delta[\delta\hat{Y}_{1k}^{in}(\Omega)]^2 \rangle = \langle \Delta[\delta\hat{Y}_{2k}^{in}(\Omega)]^2 \rangle = 1$, $(k = 1, 2, \cdots, n)$. $\hat{\beta}_j^{in} (j = 0k, 1k, 2k)$ is the vacuum noise produced by the internal loss mechanism in a NOPO, so we have $\langle \Delta[\delta\hat{X}_{\beta_{0k}}^{in}(\Omega)]^2 \rangle = \langle \Delta[\delta\hat{X}_{\beta_{1k}}^{in}(\Omega)]^2 \rangle = \langle \Delta[\delta\hat{X}_{\beta_{2k}}^{in}(\Omega)]^2 \rangle = \langle \Delta[\delta\hat{Y}_{\beta_{0k}}^{in}(\Omega)]^2 \rangle = \langle \Delta[\delta\hat{Y}_{\beta_{1k}}^{in}(\Omega)]^2 \rangle = \langle \Delta[\delta\hat{Y}_{\beta_{2k}}^{in}(\Omega)]^2 \rangle = 1$, $(k = 1, 2, \ldots, n)$. Except NOPO$_1$ $(k = 1)$, which is pumped by the coherent state of light from a laser source, all other NOPO$_k$ $(k = 2, 3, \cdots, n)$ are pumped by the thermal state of the optical field, which is the signal light produced by NOPO$_{k-1}$ before it. We will consider that except NOPO$_1$, all other NOPO$_k$ have the same physical parameters (γ, μ, γ_0, μ_0 and σ) for simplicity and not loss generality. The following results are obtained in this case.

Figure 2 shows the quantum correlation variances for $n = 4$ (S_1: $\langle \Delta(\delta\hat{X}_{22}^{out} - \delta\hat{X}_{21}^{out})^2 \rangle + \langle \Delta(\sum_{q=1}^{4} \delta\hat{Y}_{2q}^{out} + \delta\hat{Y}_{14}^{out})^2 \rangle$, S_2: $\langle \Delta(\delta\hat{X}_{23}^{out} - \delta\hat{X}_{22}^{out})^2 \rangle + \langle \Delta(\sum_{q=1}^{4} \delta\hat{Y}_{2q}^{out} + \delta\hat{Y}_{14}^{out})^2 \rangle$, S_3: $\langle \Delta(\delta\hat{X}_{24}^{out} - \delta\hat{X}_{23}^{out})^2 \rangle + \langle \Delta(\sum_{q=1}^{4} \delta\hat{Y}_{2q}^{out} + \delta\hat{Y}_{14}^{out})^2 \rangle$, S_4: $\langle \Delta(\delta\hat{X}_{24}^{out} - \delta\hat{X}_{14}^{out})^2 \rangle + \langle \Delta(\sum_{q=1}^{4} \delta\hat{Y}_{2q}^{out} + \delta\hat{Y}_{14}^{out})^2 \rangle \rangle$ vary with the analysis frequencies, where the parameters $\gamma_1 = 0.016$, $\gamma = 0.042$, $\gamma_0 = 0.4$, $\gamma_{01} = 0.15$, $\sigma_1 = 1.04$, $\sigma = 1.944$, $\mu = \mu_1 = \mu_0 = \mu_{01} = 0.001$ and the round-trip time $\tau = 3.45 \times 10^{-10} s$. It can be seen that the bright five-color entanglement can be generated from this system when the analysis frequency (f) is chosen in the range of $0.6\,\text{MHz} < f < 11\,\text{MHz}$.

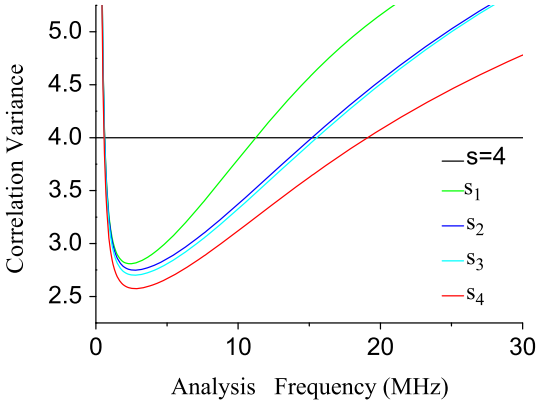

Fig. 2 The quantum correlation variance (S_1: $\langle \Delta(\delta \hat{X}_{22}^{out} - \delta \hat{X}_{21}^{out})^2 \rangle + \langle \Delta(\sum_{q=1}^{4} \delta \hat{Y}_{2q}^{out} + \delta \hat{Y}_{14}^{out})^2 \rangle$, S_2: $\langle \Delta(\delta \hat{X}_{23}^{out} - \delta \hat{X}_{22}^{out})^2 \rangle + \langle \Delta(\sum_{q=1}^{4} \delta \hat{Y}_{2q}^{out} + \delta \hat{Y}_{14}^{out})^2 \rangle$, S_3: $\langle \Delta(\delta \hat{X}_{24}^{out} - \delta \hat{X}_{23}^{out})^2 \rangle + \langle \Delta(\sum_{q=1}^{4} \delta \hat{Y}_{2q}^{out} + \delta \hat{Y}_{14}^{out})^2 \rangle$, S_4: $\langle \Delta(\delta \hat{X}_{24}^{out} - \delta \hat{X}_{14}^{out})^2 \rangle + \langle \Delta(\sum_{q=1}^{4} \delta \hat{Y}_{2q}^{out} + \delta \hat{Y}_{14}^{out})^2 \rangle\rangle$ vary with the analysis frequencies. The line of variance 4.0 is the limit of the inseparability criterion

It has been theoretically proved that in the frequency range lower than 0.6 MHz, the correlation variance is slightly sensitive to the noise existing on the each single output beam, and the good correlation is not easy obtained for the NOPO above the threshold [27]. The five-color entanglement beam does not exist when $f > 11$ MHz due to the limitation of bandwidth of NOPO cavity. There is an optimum value of the analysis frequency ($f = 3$ MHz) where the best five-color entanglement is obtained.

We can find that the quantum correlation variance of $S_1 = \langle \Delta(\delta \hat{X}_{22}^{out} - \delta \hat{X}_{21}^{out})^2 \rangle + \langle \Delta(\sum_{q=1}^{4} \delta \hat{Y}_{2q}^{out} + \delta \hat{Y}_{14}^{out})^2 \rangle$ is higher than others, and thus, if $S_1 < 4$, all others will also smaller than 4. Thus, in the following, we just give the dependences of the quantum correlation variances of S_1 on the cavity parameters. Figure 3 shows the influences of various parameters on the correlation variances when the number of cascaded NOPO is four. Figure 3a is the function of the correlation variances versus the pump parameter σ_1 of NOPO_1 and the pump parameter σ of the $NOPO_k$ ($k = 2, 3, \cdots, n$)for $\gamma_1 = 0.016$, $\gamma = 0.042$, $\gamma_{01} = 0.15$ and $\gamma_0 = 0.4$. We can see that the smaller the value of the pump parameter σ_1 of NOPO_1 is, the higher the degree of entanglement of the output five-color entangled beam is, and we cannot get the five-color entangled beam when $\sigma_1 > 2.5$. The optimum value of pump parameter of NOPO_1 should be 1.0 in principle; however, the NOPO is very unstable in this condition. So, we take the value of σ_1 to be 1.04 hereinafter. When the pump parameter of all other NOPOs is taken at $1.7 < \sigma < 2.5$, the bright five-color entanglement can be generated. The optimum value of the pump parameter σ is $\sigma = 1.944$ where the best five-color entangled light is obtained. When $\sigma < 1.5$ or $\sigma > 2.8$, the correlation variances are higher than "4", the five-color entanglement does not exist.

Figure 3b is the function of correlation variances versus the transmissivities γ_{01} and γ_0 of the input mirrors of the NOPO_1 and NOPO_k ($k = 2, 3, \cdots, n$) for the pump light with $\gamma_1 = 0.016$, $\gamma = 0.042$, $\sigma_1 = 1.04$ and $\sigma = 1.944$. It shows that the five-color entanglement cannot be obtained when the transmissivity $\gamma_0 < 0.077$. The transmissivity γ_{01} of NOPO_1 hardly affects the multicolor entanglement property.

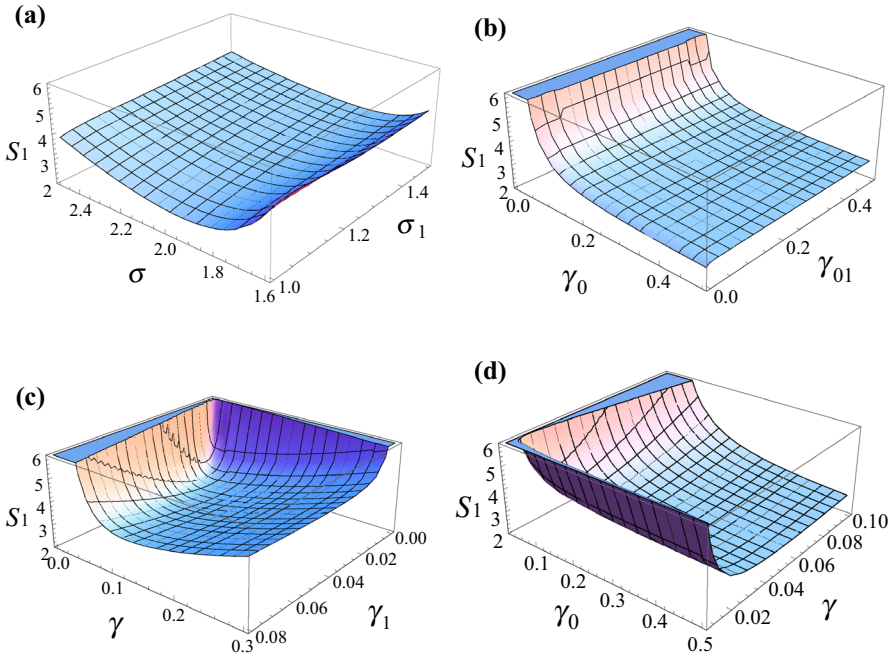

Fig. 3 The quantum correlation variances change with various parameters. **a** Correlation variance (S_1) versus the pump parameter of NOPO$_1$ (σ_1) and the NOPO$_k$ (σ); **b** correlation variance (S_1) versus the transmissivity of the input mirrors for the pump light of the NOPO$_1$ (γ_{01}) and the NOPO$_k$ (γ_0); **c** correlation variance (S_1) versus the transmissivity of the output mirrors for the signal (idler) mode of the NOPO$_1$ (γ_1) and the NOPO$_k$ (γ); **d** correlation variance (S_1) versus the transmissivity γ and the transmissivity γ_0

Figure 3c is the dependence of the correlation variances on the transmissivities γ_1 and γ of the output mirrors of the NOPO$_1$ and NOPO$_k$ ($k = 2, 3, \cdots, n$) for the signal (idler) mode with $\gamma_{01} = 0.15$, $\gamma_0 = 0.4$, $\sigma_1 = 1.04$ and $\sigma = 1.944$. It shows that the five-color entanglement cannot be generated in these regions of $\gamma < 0.009$, $\gamma > 0.25$ and $\gamma_1 < 0.001$ or $\gamma_1 > 0.07$. When $0.015 < \gamma < 0.23$, $0.004 < \gamma_1 < 0.049$, the five-color entangled state can be obtained. Taking $\gamma = 0.042$ and $\gamma_1 = 0.016$ the lowest correlation variance, i.e., the best entanglement is achieved.

Figure 3d is the dependence of the correlation variance on γ and γ_0 with $\gamma_1 = 0.016$, $\gamma_{01} = 0.15$, $\sigma_1 = 1.04$ and $\sigma = 1.944$. It shows that the five-color entanglement cannot be generated in the regions of γ and γ_0 is very small. With the increasing of γ and γ_0, the correlation variance becomes more and more smaller; when $\gamma = 0.042$ and $\gamma_0 = 0.5$, the lowest correlation variance is reached.

4 The limit of the number of cascaded NOPOs

Figure 4a–f shows the functions of the correlation variances versus the number of NOPOs for different σ, γ_1 and $f = \Omega/2\pi$, respectively, in which we take $\mu = \mu_1 = \mu_0 = \mu_{01} = 0.0005$ that are the parameters used in the experimental system of Ref. [31].

Figure 4a shows the dependence of n on σ with $\gamma_1 = 0.016$, $\gamma_{01} = 0.15$, $\gamma = 0.042$, $\gamma_0 = 0.4$, $\sigma_1 = 1.04$ and $f = 3.0\,\mathrm{MHz}$. The cascade number n firstly increases and then decreases with the increase in σ. When $\sigma = 2$ and $\sigma = 1.5$, the correlation variances are smaller than 4 for $n < 5$ and $n < 2$; i.e., we can realize six-color ($n = 5$) and three-color ($n = 2$) entanglement, respectively.

Figure 4b shows the relationship between the number n and σ_1 with $\gamma_1 = 0.016$, $\gamma_{01} = 0.15$, $\gamma = 0.042$, $\gamma_0 = 0.4$, $\sigma = 1.944$ and $f = 3.0\,\mathrm{MHz}$. It shows that the cascade number increases with the decrease in the pump parameter. The optimal value of σ_1 appears around the threshold of NOPO_1 ($\sigma_1 \sim 1$), which just is the optimal operation condition of a standard NOPO used for the generation of squeezed and entangled states [21,22,27].

Figure 4c gives the dependence of the number n on γ with $\gamma_1 = 0.016$, $\gamma_{01} = 0.15$, $\gamma_0 = 0.4$, $\sigma_1 = 1.04$, $\sigma = 1.944$ and $f = 3.0\,\mathrm{MHz}$. The cascade number first increases and then decreases with the increase in the transmissivity γ. When $\gamma = 0.02$ and $\gamma = 0.042$, the maximal cascaded number of NOPOs for generating multicolor entanglement is $n = 4$ and $n = 5$, respectively. However, if the value of γ is higher than 0.042, the possible number of cascaded NOPOs will decrease, and thus, the six-color entanglement is the obtainable largest-size entangled state under above given parameter condition.

Figure 4d shows the dependence of the limit n on γ_1 with $\gamma_{01} = 0.15$, $\gamma_0 = 0.4$, $\gamma = 0.042$, $\sigma_1 = 1.04$, $\sigma = 1.944$ and $f = 3.0\,\mathrm{MHz}$. Similarly, the cascade number firstly increases and then decreases with the increase in γ_1. An optimal γ_1 can be found for a given system.

Figure 4e shows the dependence of the number n on γ_0 with $\gamma_1 = 0.016$, $\gamma_{01} = 0.15$, $\gamma = 0.042$, $\sigma_1 = 1.04$, $\sigma = 1.944$ and $f = 3.0\,\mathrm{MHz}$. It shows that the higher the γ_0 is, the better the entanglement among the output beams is, and the more the cascade number is. However, when transmission of the input mirror is higher, the required pump power is also higher. When $\gamma_0 > 0.5$, the possible number of cascaded NOPOs almost does not increase, and thus, the value of γ_0 may be choose about 0.5 which is easily realized in the experiment.

Figure 4f shows that the number n varies with the analysis frequencies f for $\gamma_1 = 0.016$, $\gamma_{01} = 0.15$, $\gamma = 0.042$, $\gamma_0 = 0.4$, $\sigma_1 = 1.04$ and $\sigma = 1.944$. The cascade number of the NOPOs decreases with the increase in the measured frequencies. Thus, due to the limitation of the bandwidth of the NOPO cavity, the measured frequency should be selected in a optimal region.

5 Summary

In conclusion, we design a generation system of CV multicolor entangled states in which multiple cascade NOPOs are used. The quantum entanglement characteristics among the resultant submodes are theoretically analyzed. Based on the inseparability criterion proposed by van Loock and Furusawa, the dependences of the correlation variances on the system parameters are numerically calculated. We also comprehensively consider the interconnection among the physical parameters of the cascade NOPOs and find the optimal operation condition for generating multicolor entanglement. The

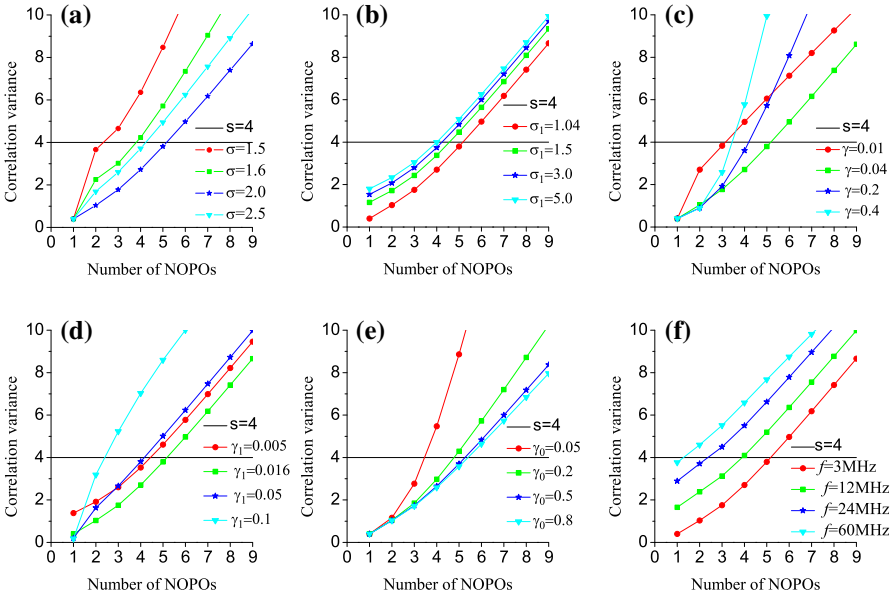

Fig. 4 Entanglement versus number of NOPOs under different experimental parameters [**a** the pump parameter σ; **b** the pump parameter σ_1; **c** the transmissivity γ; **d** the transmissivity γ_1; **e** the transmissivity γ_0; **f** the measurement frequencies f]. The line of variance 4.0 is the limit of the inseparability criterion

results calculated based on the physical parameters used in really experimental systems provide valuable references for designing multicolor entanglement generation systems of optical modes.

Acknowledgments W. Liu thanks K. Peng, C. Xie and X. Su for the helpful guidance. This research was supported by the Foundation for University Key Teacher by the Ministry of Education of China, Natural Science Foundation of China (Grants Nos. 11322440, 11474190 and 61121064), FOK YING TUNG Education Foundation and the Special Research Plan Project of Education Department of Shaanxi Province (Grants No. 11JK0547).

References

1. Einstein, A., Podolsky, B., Rosen, N.: Can quantum-mechanical description of physical reality be considered complete? Phys. Rev. **47**, 777 (1935)
2. Bell, J.S.: On the Einstein Podolsky Rosen paradox. Physics **1**, 195–200 (1964)
3. Nielsen, M.A., Chuang, I.L.: Quantum Computation and Quantum Information. Cambridge University Press, Cambridge (2000)
4. Haroche, S., Raimond, J.-M.: Exploring the Quantum. Oxford University Press, Oxford (2006)
5. Furusawa, A., Søensen, J.L., Braunstein, S.L., Fuchs, C.A., Kimble, H.J., Polzik, E.S.: Unconditional quantum teleportation. Science **282**, 706–709 (1998)
6. Lance, A.M., Symul, T., Bowen, W.P., Sanders, B.C., Lam, P.K.: Tripartite quantum state sharing. Phys. Rev. Lett. **92**, 177903 (2004)
7. Honda, K., Akamatsu, D., Arikawa, M., Yokoi, Y., Akiba, K., Nagatsuka, S., Tanimura, T., Furusawa, A., Kozuma, M.: Storage and retrieval of a squeezed vacuum. Phys. Rev. Lett. **100**, 093601 (2008)
8. Appel, J., Figueroa, E., Korystov, D., Lobino, M., Lvovsky, A.I.: Quantum memory for squeezed light. Phys. Rev. Lett. **100**, 093602 (2008)

9. Jia, X., Su, X., Pan, Q., Gao, J., Xie, C., Peng, K.: Experimental demonstration of unconditional entanglement swapping for continuous variables. Phys. Rev. Lett. **93**, 250503 (2004)
10. Atature, M., Dreiser, J., Badolato, A., Hoele, A., Karrai, K., Imamoglu, A.: Quantum-dot spin-state preparation with near-unity fidelity. Science **312**, 551–553 (2006)
11. Leibfried, D., Knill, E., Seidelin, S., Britton, J., Blakestad, R.B., Chiaverini, J., Hume, D.B., Itano, W.M., Jost, J.D., Langer, C., Ozeri, R., Reichle, R., Wineland, D.J.: Creation of a six-atom 'Schrodinger cat' state. Nature **438**, 639–642 (2005). (London)
12. Kimble, H.J.: The quantum internet. Nature **453**, 1023–1030 (2008). (London)
13. Su, X., Tan, A., Jia, X., Zhang, J., Xie, C., Peng, K.: Experimental preparation of quadripartite cluster and Greeberger–Horne–Zeilinger entangled states for continuous variables. Phys. Rev. Lett. **98**, 070502 (2007)
14. Yukawa, M., van Ukai, R., Loock, P., Furusawa, A.: Experimental generation of four-mode continuous-variables cluster states. Phys. Rev. A **78**, 012301 (2008)
15. Allevi, A., Bondani, M., Paris, M.G.A., Andreoni, A.: Demonstration of a bright and source of tripartite nonclassical light. Phys. Rev. A **78**, 063801 (2008)
16. Villar, A.S., Cruz, L.S., Cassemiro, K.N., Martinelli, M., Nussenzveig, P.: Generation of bright two-color continuous variable Entanglement. Phys. Rev. Lett. **95**, 243603 (2005)
17. Su, X., Tan, A., Jia, X., Pan, Q., Xie, C., Peng, K.: Experimental demonstration of quantum entanglement between frequency-nondegenerate optical twin beams. Opt. Lett. **31**, 1133–1135 (2006)
18. Jing, J., Feng, S., Bloomer, R., Pfister, O.: Experimental continuous-variable entanglement from a phase-difference-locked optical parametric oscillator. Phys. Rev. A **74**, 041804(R) (2006)
19. Keller, G., D'Auria, V., Treps, N., Coudreau, T., Laurat, J., Fabre, C.: Experimental demonstration of frequency-degenerate bright EPR beams with a self-phase-locked OPO. Opt. Express **16**, 9351–9356 (2008)
20. Li, Y., Guo, X., Bai, Z., Liu, C.: Generation of two-color continuous variable quantum entanglement at 0.8 and 1.5m. Appl. Phys. Lett. **97**, 031107 (2010)
21. Coelho, A.S., Barbosa, F.A.S., Cassemiro, K.N., Villar, A.S., Martinelli, M., Nussenzveig, P.: Three-color entanglement. Science **326**, 823–826 (2009)
22. Jia, X., Yan, Z., Duan, Z., Su, X., Wang, H., Xie, C., Peng, K.: Experimental realization of three-color entanglement at optical fiber communication and atomic storage wavelengths. Phys. Rev. Lett. **109**, 253604 (2012)
23. Villar, A.S., Martinelli, M., Fabre, C., Nussenzveig, P.: Direct production of tripartite pump-signal-idler entanglement in the above-threshold optical parametric oscillator. Phys. Rev. Lett. **97**, 140504 (2006)
24. Tan, A., Xie, C., Peng, K.: Bright three-color entangled state produced by cascaded optical parametric oscillators. Phys. Rev. A **85**, 013819 (2012)
25. Tan, A.: Multi-color continuous-variable entangled optical beams generated by NOPOs. Quantum Inf. Process. **12**, 3275 (2013)
26. Wang, D., Zhang, Y., Xiao, M.: Quantum limits for cascaded optical parametric amplifiers. Phys. Rev. A **87**, 023834 (2013)
27. Fabre, C., Giacobino, E., Heidmann, A., Raynaud, S.: Noise characteristics of a non-degenerate optical parametric oscillator-application to quantum noise reduction. J. Phys. (France) **50**, 1209 (1989)
28. van Loock, P., Furusawa, A.: Detecting genuine multipartite continuous-variable entanglement. Phys. Rev. A **67**, 052315 (2003)
29. Simon, R.: PeresCHorodecki separability criterion for continuous variable systems. Phys. Rev. Lett. **84**, 2726 (2000)
30. Werner, R.F., Wolf, M.M.: Bound entangled Gaussian states. Phys. Rev. Lett. **86**, 3658 (2001)
31. Mehmet, M., Ast, S., Eberle, T., Steinlecher, S., Vahlbruch, H., Schnabel, R.: Squeezed light at 1550nm with a quantum noise reduction of 12.3 dB. Optics Express **19**, 25763–25772 (2011)